

Spherical indentation of tooth enamel

M. STAINES, W. H. ROBINSON

Physics and Engineering Laboratory, DSIR, Lower Hutt, New Zealand

J. A. A. HOOD

School of Dentistry, University of Otago, Dunedin, New Zealand

Spherical indentation measurements were made on enamel surfaces of intact human teeth. From the load versus depth of indentation curve Young's modulus was found to be typically 8.3×10^{10} Pa and the yield stress to be 3.3×10^8 Pa. Young's modulus was observed to vary with moisture content and with the orientation of the enamel surface. Viscoelastic behaviour was evident, also depending on the moisture content of the enamel.

1. Introduction

Spherical indentation resulting in plastic deformation is widely used in the form of the Brinell hardness test. It has been less often used to study the elastic properties of materials by utilizing Hertz's solution for the elastic contact of spherical bodies [1]. For the indentation of a semi-infinite isotropic medium by a spherical ball his result predicts that the combined ball and specimen elastic deformation is

$$h = \frac{[(1 - \nu_b^2)/E_b + (1 - \nu_s^2)/E_s]^{2/3}}{(9/8D)^{1/3} F^{2/3}} \quad (1)$$

where ν_b and ν_s are Poisson's ratios, E_b and E_s are Young's moduli for the ball and specimen, respectively, D is the ball diameter and F is the applied load. In the limit of an infinitely stiff ball, h is simply the penetration depth. For a tungsten carbide ball indenting a typical enamel specimen the penetration depth is about $0.92h$. Using the relation above $E_s(1 - \nu_s^2)^{-1}$ can be determined from the force–displacement curve for an elastic indentation. E_s can be calculated from this quantity with relatively little sensitivity to uncertainty in ν_s ; even if ν_s is unknown the assumption that it equals $(2\sqrt{2})^{-1}$ determines E_s to within $\pm 12.5\%$ [2]. Even when considerable plastic deformation has taken place on loading, the unloading curve records only elastic recovery allowing Young's modulus to be calculated [3, 4].

Indentation tests have the virtues of involving minimal specimen preparation or damage and of producing large stresses concentrated in a small volume. This enables measurements to be made on small specimens as in the work of Cousins *et al.* on lignin [2] and the present work on the enamel of intact human teeth. Furthermore, the method simulates the natural loading of enamel thus ensuring that the observed behaviour of the material is relevant to its function.

The elastic properties of enamel are relevant to the behaviour of this tissue under masticatory load. They have been measured previously by Craig *et al.* [5] using compressive loading. A number of studies have been made using ultrasonic techniques, most recently by Grenoble *et al.* [6] and Gilmore *et al.* [7]. The value of Young's modulus obtained in the present study was in good agreement with these results. Moreover, we have observed dependence of the elastic properties on moisture content, orientation and rate of strain. Before describing the experimental method and results, we briefly mention some relevant facts about enamel.

Enamel is a composite material, consisting of about 87 vol% mineral, nominally hydroxyapatite, $\text{Ca}_5(\text{PO}_4)_3\text{OH}$, 2% organic component and 11% water [8]. It is constructed of closely fitting prisms, with transverse dimensions about $5 \mu\text{m}$, running roughly perpendicular to the surface through the depth of the enamel, roughly 1 mm.

Within each prism crystallites of hydroxyapatite (typical dimensions 30 nm × 70 nm × 400 nm) [9] are oriented generally along the prism but diverging somewhat towards its boundary. The disposition of the organic component, whether as embedded fibrils or as a matrix or prism sheath, is subject to debate [10].

2. Experimental procedure

The indenter assembly was the same as that used by Robinson and Truman [4], consisting of a 6.35 mm diameter tungsten carbide ball and two internally mounted displacement transducers (Mercer model 490) as shown in Fig. 1. The assembly was fixed to a 5 kN load cell on the cross-head of a model TT-K Instron testing machine. The combined depth of penetration and deformation of the ball were obtained from the displacement transducers whose probes contacted the specimen mounting block 7.5 mm either side of the ball. Any effects due to tilting of the specimen were cancelled by taking the average reading of the transducers. Reproducibility of the displacement was $\pm 0.01 \mu\text{m}$. Force displacement curves were recorded on an X-Y recorder. Indentations were made at cross-head speeds varying from 1 to $100 \mu\text{m min}^{-1}$.

The specimens were sound, intact human teeth mounted in 25 mm diameter epoxy blocks. The end surfaces of the blocks were hand lapped, using Griffin 5-20 and 3-50 alumina and finishing with fine γ -alumina, to expose an area of enamel a few millimetres square. The specimens were kept

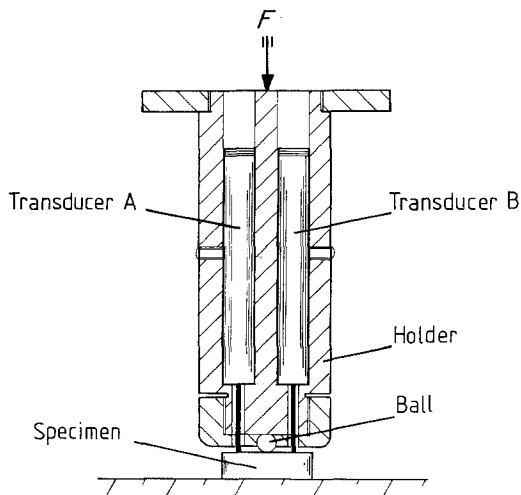


Figure 1 Schematic diagram of indenter showing transducers.

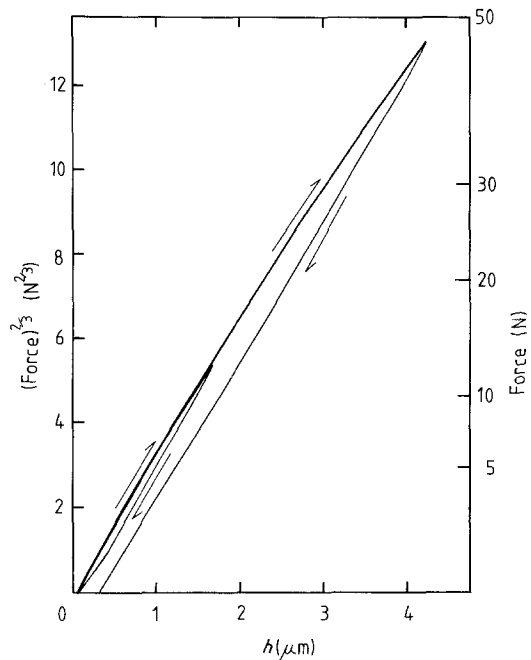


Figure 2 Force^{2/3} against displacement curve for initial indentations of side enamel.

in water until testing. The indentation was made within about 0.1 mm of the desired site by positioning the specimen, with the aid of a microscope, above a reference mark made by the indenter on the anvil. A series of comparative measurements, as when investigating the effect of changes in indentation rate and enamel moisture content, could be carried out over a fixed indentation range without shifting the specimen. One could therefore be confident any changes were not due to spatial variation of the elastic properties of the specimen. In favourable cases the modulus was reproducible to within about 1%.

3. Results and discussion

Fig. 2 shows typical results of $F^{2/3}$ versus h for the initial indentation of a specimen of side enamel at a cross-head speed of $20 \mu\text{m min}^{-1}$. It is apparent that no plastic deformation has occurred on the initial loading to a depth of $1.6 \mu\text{m}$ since the reloading curve coincides with the loading curve. The different path for unloading shows that dental enamel is viscoelastic. A series of viscoelastic loading-unloading loops is seen in the continuation of the measurements on the same specimen in Fig. 3. Considerable plastic deformation is evident. A dent $17 \mu\text{m}$ deep was left at the completion of the measurements.

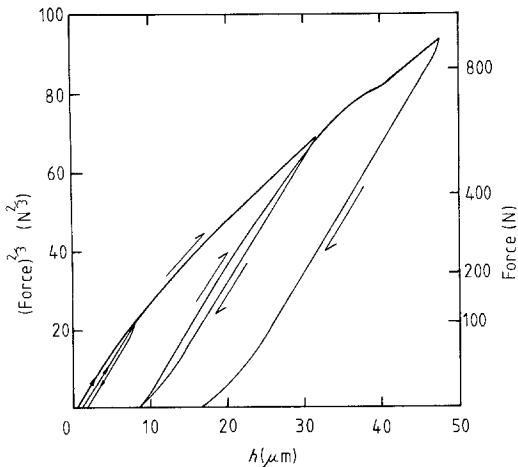


Figure 3 Force^{2/3} against displacement curve for indentations of enamel after loading in Fig. 2.

Similar hysteresis loops were found by Fox [11] in measurements involving much larger deformation (~ 0.5 mm) in which a distributed load was applied by a 3 mm diameter ball lying in the cusp of the tooth.

3.1. Brittle–plastic behaviour

Circular cracks centred on the indentation site were generally observed after a test cycle such as that of Fig. 3. Cone fractures of this type are a feature of the spherical indentation of brittle materials such as glass and ceramics, forming at the perimeter of the contact zone between indenter and specimen when the radial stress exceeds the tensile strength of the material. However, the present measurements yield no information about the fracture mechanics of enamel because the onset of cracking has no conspicuous effect on the force–displacement curves.

Non-circular cracks were also commonly observed after deep indentations and obviously occurred at planes of weakness in the enamel structure, possibly enamel lamellae [12].

In ductile materials, such as metals, permanent indentations result from plastic flow beginning at the point of maximum shear stress at a depth about half the radius of contact below the ball. Theory predicts that the yield stress is about 92% of the mean pressure under the ball at the beginning of plastic flow [13]. Thus for the enamel specimen in Fig. 3 for which plasticity begins at a penetration of about $2 \mu\text{m}$ the estimated yield stress is 3.7×10^8 Pa. The mean value for our specimens was $3.3 \pm 0.4 \times 10^8$ Pa.

In the course of their indentation studies of metals, Robinson and Truman [3] developed definitions of stress and strain appropriate to the interpretation of force versus depth of indentation measurements. This allows stress–strain curves to be drawn and the work-hardening and yield characteristics of diverse materials to be compared. However, one must know the radius of curvature of the permanent indentation remaining after each loading. In the case of metals this was found from the increase in slope of the $F^{2/3}$ against h plot. This has not been possible with enamel because generally for deep indentations ($h > 10 \mu\text{m}$) the unloading curves were not Hertzian ($h \propto F^{2/3}$) so that it was not possible to detect any clear trend in the slopes of the successive curves. This is most likely due to the effects of viscoelasticity, cracking and inhomogeneity of the enamel.

3.2. Viscoelastic behaviour

For a given depth of indentation the width of the loading–unloading loop for cyclic indentations provided a simple measure of the magnitude of viscous damping in the enamel. Within the experimental range of indentation rates (1 to $100 \mu\text{m min}^{-1}$) the loop width varied inversely with the rate of indentation. This established that the mean relaxation time for the dominant mechanism of viscous damping was greater than the time taken for a loading–unloading cycle, which was up to several minutes.

Natural drying of the tooth in air caused a significant reduction in the loop width. For example a particular specimen of cusp enamel indented at $50 \mu\text{m min}^{-1}$ had a loop width, expressed as a fraction of the indentation depth, of 3.4% when wet. After 16 h in air this was reduced to 2.3%, recovering slightly to 2.5% 2 h after rewetting. This suggests that the viscous damping may be due to the pumping of fluids in spaces within the enamel [11]. If this is the case, indentation measurements may provide a convenient means of studying the transport of fluid in the enamel—possibly an important factor in the development of carious lesions in the enamel [14].

3.3. Young's modulus

The slope of the unloading sections of the $F^{2/3}$ against h plots of Figs 2 and 3 is indicative of a Young's modulus of 8.0×10^{10} Pa, assuming a

TABLE I Young's modulus of dental materials

Reference	Material	Young's modulus ($\times 10^{10}$ Pa)
Indentation measurements (present work)		8.3 \pm 0.8
Compression tests	{ Cusp enamel Side enamel	8.4 \pm 0.6
Craig <i>et al.</i> [5]		7.8 \pm 0.5
Ultrasonic measurements	{ Bovine enamel	7.7
Grenoble <i>et al.</i> [6]	{ Synthetic hydroxyapatite	11.7
Gilmore <i>et al.</i> [7]	{ Bovine enamel	7.4

Poisson's ratio of 0.23 obtained from ultrasonic measurements on bovine enamel in the longitudinal direction [6]. The true quasi-static Poisson's ratio may differ somewhat from this value with a minor effect on the calculated modulus. The mean value over 30 measurements at different sites on eight teeth was 8.3×10^{10} Pa, with a standard deviation of 0.8×10^{10} Pa. In fact the results were not normally distributed, with a few extreme results ranging from 6.9 to 13.6×10^{10} Pa. There was no clear correlation with tooth type or indentation site and the specimens with extreme moduli had no distinctive features. Table I compares this result with those obtained by other workers for enamel and hydroxyapatite. The variability of our results meant we were unable to confirm the slight difference in modulus between cusp and side enamel detected by Craig *et al.* [5].

It is likely that the spread of values for Young's modulus mainly reflects variations in the degree of mineralization of the enamel. One can estimate the sensitivity of E to the volume concentration of hydroxyapatite as follows. It is plain, from Katz's [15] discussion of the elastic properties of simple models of hard tissue composites that one can expect Young's modulus to change linearly from 8.1×10^{10} Pa typical of enamel, with 87% volume concentration hydroxyapatite, to the 11.7×10^{10} Pa measured for pure hydroxyapatite. Young's modulus must then change by 0.3×10^{10} Pa for each percentage change in the volume concentration of hydroxyapatite. Thus a standard deviation of only 3% in the degree of mineralization is consistent with the experimental results. This argument is strictly correct only for pure hydroxyapatite with a Ca/P ratio of 1.67, the Ca/P ratio for enamel mineral varies about this ideal value [16]. Clearly, measurements of both Young's modulus and the degree of mineralization are required to conclusively establish the connection.

The measured Young's modulus was affected, like the width of the hysteresis loop, by loss of

moisture from the enamel. The data of Table II shows the modulus of a specimen of side enamel increased by some 15% after 72 h drying at room temperature. Presumably the lack of recovery after rewetting simply meant that insufficient time was allowed for rehydration. It is unlikely that this increase in E is caused by stiffening of the organic component due to dehydration—as Katz [15] pointed out, the elastic modulus of highly mineralized hard tissue is only weakly dependent on that of the organic component. It may be that shrinkage and the loss of water from voids are more significant factors.

Finally, we observed differences in Young's modulus measured at different sites on a single facet of side enamel which may reflect the structural anisotropy of enamel. The three neighbouring sites are shown schematically in Fig. 4. At Sites 1 and 2 the indentations are roughly co-axial with the enamel prisms and thus, on average, parallel to the c -axis of the hydroxyapatite crystals. At Site 3 the indentation is more nearly perpendicular to the c -axis of the crystals. The experimental values of Young's modulus obtained from unloading $2 \mu\text{m}$ deep indentations at these sites are listed in Table III. The transverse indentation yields a modulus some 20% higher than the others. It might be argued that the elastic modulus varies with depth, since different levels of enamel were exposed on the polished facet. The similar results at Sites 1 and 2 argue against this possibility.

There are a number of reasons why these results should be regarded as provisional until a system-

TABLE II Variation of Young's modulus of enamel with moisture content

Moisture content	Young's modulus ($\times 10^{10}$ Pa)
Wet	6.9
18 h drying in air	7.8
72 h drying in air	8.0
2 h after wetting	8.0

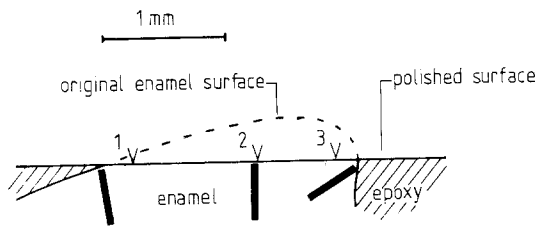


Figure 4 Schematic diagram of enamel specimen. The three indentation sites are shown. The solid bars within the enamel suggest the orientation of the enamel prisms.

matic investigation has been undertaken. Because of surface geometry this type of comparison was possible with only one of the specimens. The degree of orientation in the specimen was not well defined. The results were interpreted using Equation 1 which is strictly correct only for isotropic materials. The transverse modulus, E , was higher than Young's modulus for pure polycrystalline hydroxyapatite (see Table I). In spite of these reservations, some comments are justified on the implications for current ideas of the structural organization of enamel.

Firstly, these results throw doubts on the "sheath" model of enamel on the grounds that the experimentally measured elastic anisotropy is opposite to, and far smaller than, the predictions of the model. Histological studies of enamel have been interpreted, with some disagreement [10], as showing organic sheaths enclosing the mineral prisms mentioned in Section 1. If the sheaths exist one would expect the compliant organic material to markedly reduce the modulus for transverse indentations while altering the modulus for parallel indentations only slightly from that for the mineral component. Model calculations [17] predict that the ratio of Young's moduli E_p/E_t for such a composite enamel would lie between 3.2 and 4.2. Our experimental result

TABLE III Dependence of elastic moduli on orientation

Orientation	Modulus ($\times 10^{10}$ Pa)
Indentation measurements ^a :	
Site 1	10.8
Site 2	11.2
Site 3	13.6
Average compliances ^b :	
Parallel S_{33}^{-1}	11.7
Transverse S_{11}^{-1}	11.2

^a See Fig. 4 for site positions.

^b Data from Tan [18].

of 0.8 suggests that the model is invalid—the organic component of enamel does not constitute a matrix in which the mineral prisms are embedded.

On the other hand, if the elastic properties of the hydroxyapatite alone are considered to be relevant a discrepancy with experiment still exists. For a uniaxial polycrystalline aggregate of hydroxyapatite with random orientation about the c -axis the single crystal compliance data [18] give $E_p/E_t = s_{11}/s_{33} = 1.04$ (see Table III). (The uniform strain (Voigt) and uniform stress (Reuss) constraints give the same result for the transverse modulus: $\langle s_{11} \rangle^{-1} = \langle s_{11}^{-1} \rangle = s_{11}^{-1}$.) The lower experimental result of 0.8 may indicate that the organic material in enamel is disposed in some way which renders the enamel more compliant to stresses normal to its surface rather than transverse.

4. Conclusions

This work has demonstrated that spherical indentation is an accurate and convenient measurement technique well suited to studying the elastic properties of biomaterials. Relative measurements, performed without relocating the indenter, are particularly useful for studying effects such as those due to dehydration. We have found that dental enamel is a visco-elastic, plastic-brittle material with typical Young's modulus of 8.3×10^{10} Pa and yield strength of 3.3×10^8 Pa. Young's modulus was observed to increase by some 15% on drying of the enamel and to depend on the orientation of the indentation with respect to the direction of enamel prisms in a way contrary to that expected of prism sheaths. The dependence of the viscoelastic behaviour on moisture content suggested the technique may have an application to the study of fluid transport in enamel.

References

1. H. R. HERTZ, "Miscellaneous Papers" (Macmillan, London 1896) Chs. 5, 6.
2. W. J. COUSINS, R. W. ARMSTRONG and W. H. ROBINSON, *J. Mater. Sci.* **10** (1975) 1655.
3. W. H. ROBINSON and S. D. TRUMAN, *ibid.* **12** (1977) 1961.
4. *Idem*, unpublished work (1980).
5. R. G. CRAIG, F. A. PEYTON and D. W. JOHNSON, *J. Dent. Res.* **40** (1961) 936.
6. D. E. GRENOBLE, J. L. KATZ, K. L. DUNN, R. S. GILMORE and K. L. MURTY, *J. Biomed. Mater. Res.* **6** (1972) 221.
7. R. S. GILMORE, R. P. POLLACK and J. L. KATZ, *Arch. Oral Biol.* **15** (1969) 787.
8. F. BRUDEVOLD and R. SOREMARK, in "Struc-

- tural and Chemical Organisation of Teeth", Vol. 2, edited by A. G. W. Miles (Academic Press, New York and London, 1967) p. 247.
9. G. DACULSI and B. KEREBEL, *J. Ultrastruct. Res.* **65** (1978) 163.
 10. J-G. HELMCKE, in "Structural and Chemical Organisation of Teeth", Vol. 2, edited by A. G. Miles (Academic Press, New York and London, 1967) p. 135.
 11. P. G. FOX, *J. Mater. Sci.* **15** (1980) 3113.
 12. G. GUSTAFSON and A-G. GUSTAFSON, in 'Structural and Chemical Organisation of Teeth', Vol. 2, edited by A. G. W. Miles (Academic Press, New York and London, 1967) p. 75.
 13. S. P. TIMOSHENKO and J. N. GOODIER, "Theory of Elasticity", 3rd ed. (McGraw-Hill, New York, 1970) p. 409.
 14. D. J. HAINES, *J. Biomechanics* **1** (1968) 117.
 15. J. L. KATZ, *ibid.* **4** (1971) 455.
 16. F. C. BESIC, C. R. KNOWLES, M. R. WEIMANN and O. KELLER, *J. Dent. Res.* **48** (1969) 131.
 17. J. J. ZYBERT, W. A. RACHINGER, P. P. PHAKEY and H. J. ORAMS, *Composites* **11** (1980) 175.
 18. S. K. TAN, quoted by R. F. S. Hearmon in "Landolt-Bornstein, New Series III/II" (Springer-Verlag, Berlin, 1979) p. 39.

Received 25 November 1980 and accepted 19 March 1981.